CYCLIC ELASTOPLASTIC LARGE DISPLACEMENT BEHAVIOUR OF STEEL COMPRESSION MEMBERS

Iraj H. P. MAMAGHANI*, Tsutomu USAMI**, and Eiji MIZUNO ***

*Member of JSCE, Doctoral Student, M. Eng., Dept. of Civil Eng., Nagoya University (Chikusa-ku, Nagoya 464-01, JAPAN)
**Member of JSCE, Dr. of Eng., Dr. SC., Professor, Dept. of Civil Eng., Nagoya University (Chikusa-ku, Nagoya 464-01, JAPAN)
***Member of JSCE, Ph. D., Associate Professor, Dept. of Civil Eng., Nagoya University (Chikusa-ku, Nagoya 464-01, JAPAN)

The present paper is concerned with the cyclic elastoplastic large displacement behaviour of steel compression members, such as pin-ended columns and cantilever type of box columns modeling bracing members and bridge piers. An elastoplastic finite element formulation for beam-columns was developed and implemented in the computer program FEAP used in the analysis. The geometrical nonlinearity is described by the modified approximate updated Lagrangian description of motion and the two-surface plasticity model is employed for material nonlinearity. The formulation accounts for the important cyclic characteristics of structural steel, even within the yield plateau, such as, the decrease and disappearance of the yield plateau, reduction of the elastic range and cyclic strain hardening as well as the spread of plasticity across the section and along the member length. The cyclic elastoplastic performance of the formulation was found to be good when compared with the experimental results and the results obtained from other material models.

Key Words : *elastoplastic, cyclic loading, hysteretic behaviour, large displacement, analysis, two-surface plasticity model, finite element, columns, energy absorption capacity*

1. INTRODUCTION

An accurate cyclic analysis of steel structures requires precise methods to predict the inelastic large displacement response of structural members such as bracing members and columns. This has been the subject of intensive research work and a variety of analytical methods were developed to simulate the hysteretic behaviour of steel members in the past few decades[1)-9)].

The main research approaches used for the cyclic analysis of columns may be classified as: empirical (phenomenological) models[3)], plastic-hinge models[2),4)] and elastoplastic finite element models[7)]. Although the empirical and plastic-hinge models can provide a good insight into the basic hysteretic behaviour of a structure, a crucial drawback involved in these methods is the neglect of gradual plastification across the cross-section and along the member length, the Bauschinger effect, cyclic strain hardening and residual stresses produced during hysteretic plastic deformation which are important factors in the overall response of the member[4)].

The more accurate models were based on finite element method considering geometric and material nonlinearities[7)]. This method is generally applicable to many types of problems, and it requires only the member geometry and material properties (constitutive law) to be defined.

Recently, various stress-strain relationships were employed in the analysis by different researchers, such as elastic-perfectly plastic, bilinear with hardening, and trilinear with both strain hardening and Bauschinger effect[8)]. From these studies, it was concluded that the spread of plas-

ticity along the length and the Bauschinger effect cause a reduction in the load carrying capacity under cyclic loading[6]. On the other hand, stress-strain relationship used in structural analyses depends on the loading history to which the structure or structural members are subjected. Therefore, an accurate and refined constitutive law should be used to account for the general cyclic behaviour of structural steel which has a characteristic yield plateau followed by strain hardening. For this purpose, based on the experimentally observed cyclic behaviour of structural steel, a multiaxial two-surface plasticity model (2SM) was recently developed by the authors[10),11),12)]. This model can treat accurately the cyclic behaviour of structural steel even within the yield plateau, such as the reduction and disappearance of the yield plateau, Bauschinger effect and cyclic strain hardening.

The main objective of this study is to apply the 2SM developed for material nonlinearity to trace cyclic elastoplastic large displacement behaviour of steel compression members, such as pin-ended columns modeling bracing members and cantilever type of steel box columns modeling bridge piers. An elastoplastic finite element formulation for beam-column, considering geometrical and material nonlinearities, was developed and implemented in the computer program FEAP[13)] used in the analysis[1)]. The modified approximate updated Lagrangian description (AULD) of motion[14)] is adopted in the element formulation for geometrical nonlinearity.

In what follows, first the important characteristics of the uniaxial 2SM, numerical procedures and solution scheme are briefly presented. Then, the cyclic plasticity performance of the formulation is compared with experiments [15),16)] as well as with results obtained from the elastic-perfectly plastic (EPP), isotropic hardening (IH) and kinematic hardening (KH) material models.

The effect of initial residual stress and initial deflection on the cyclic behaviour of steel columns are examined using the developed formulation. It is found that the initial residual stress and increase in the initial deflection have only the effect of decreasing the initial buckling load capacity and do not affect subsequent cyclic behaviour.

It is shown that the developed formulation can predict with a high degree of accuracy the experimentally observed cyclic behaviour of axially loaded pin-ended columns and steel box columns of cantilever type. Therefore, it can be used in the nonlinear structural analysis; to generate parametric data; and to check the accuracy of the more simplified models.

2. UNIAXIAL TWO-SURFACE MODEL

In the beam-column element formulation, the cyclic constitutive law for structural steels is described by the uniaxial 2SM developed based on the originally proposed by Dafalias and Popov[17)], and the experimentally observed cyclic elastoplastic behaviour of structural steel grades SS400, SM490 and SM570[10),11),12)]. The important characteristics of the uniaxial 2SM, shown schematically in Fig. 1, are briefly reviewed as follows:

1. The plastic modulus E^P, is expressed as:

$$E^P = \frac{d\sigma}{d\varepsilon^p} = E_0^P + \beta \frac{\delta}{\delta_{in} - \delta} \qquad (1)$$

where, E_0^P is the slope of the current bounding line; δ is the distance between the bounding line and loading point (say, point Q_2 in Fig. 1) and is assumed always greater than or equal to zero; δ_{in} is the value of δ at the initial yield state in the current loading path (say, point Q_1 for path CD in Fig. 1); β is called the shape parameter and is assumed to be a linear function of δ as follows:

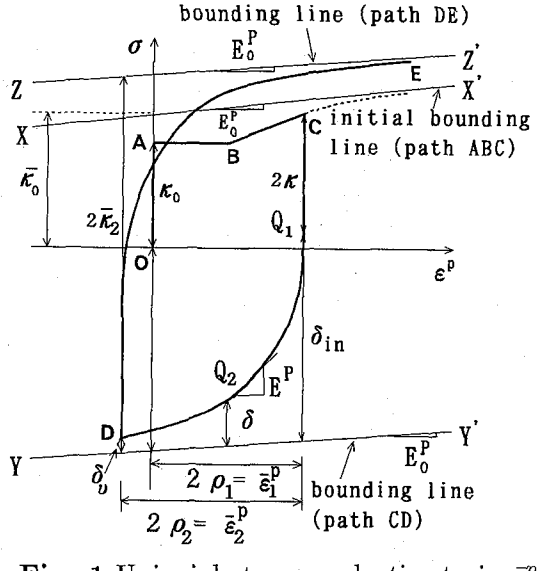

Fig. 1 Uniaxial stress σ-plastic strain $\bar{\varepsilon}^p$ curve

$$\beta = e \cdot \delta + f \qquad (2)$$

where e and f are material constants.

2. The Bauschinger effect (reduction of the elastic range) is expressed as a function of the effective plastic strain (EPS) range (denoted as AEPS by Shen et al.[10]), which is defined as the maximum amplitude of the effective plastic strain that the material has ever experienced[18].
3. The prediction of the end of yield plateau is important in the evaluation of cyclic behaviour. Based on monotonic and cyclic experimental results, the disappearance of the yield plateau is treated depending on the EPS range and the plastic work.
4. In order to accurately predict the cyclic strain hardening, the movement of the bounding lines is introduced in the uniaxial 2SM. The size of the bounding lines, $\bar{\kappa}$, is defined as a function of the EPS range, $\bar{\varepsilon}^p$ as shown in Fig. 1. The limiting value of the size of bounding lines is assumed to be equal to the tensile ultimate stress σ_u, with the increase in the plastic deformation[12].
5. The virtual bounding line and memory line concepts are used to improve the accuracy of the model when cycling is random and the reversed loading point does not reach the memory line.
6. The slope of the bounding line, E_0^P in Fig. 1, is assumed to decrease with the plastic work.

It is worth noting that, in the uniaxial 2SM model, all the parameters are obtained from experimental data under relatively simple loading histories[10]. The material properties and model parameters for different steel grades, obtained by the authors, are listed in Table 1, where E, σ_y, ν, and ε_{st}^p denote the Young's modulus, yield stress, Poisson's ratio and length of yield plateau for the material, respectively. The other notations in Table 1 are related to the model parameters and explained in detail in references 10) and 12). The accuracy of the 2SM has already been verified by the experimental data[10),11),12].

Table 1 Material properties and 2SM parameters for steel grades SS400, SM490 and SM570

Parameter	SS400	SM490	SM570
$E(GPa)$	207	206	216
$\sigma_y(MPa)$	274	357	524
ν	0.29	0.25	0.25
E_{st}^p/E	2.49×10^{-2}	3.40×10^{-2}	1.02×10^{-2}
$\varepsilon_{st}^p/\varepsilon_y$	12.0	7.0	0.00
a	-0.505	-0.528	-0.553
b	2.17	1.88	6.47
c	14.4	18.7	34.8
α	0.191	0.217	0.175
e	5.00×10^{2}	3.16×10^{2}	7.00×10^{2}
f/E	0.30	0.484	0.361
M	-0.37	-0.522	—
E_0^P/E	8.96×10^{-3}	1.01×10^{-2}	7.85×10^{-3}
$\omega \cdot \sigma_y$	3.08	4.0	2.67
$\bar{\kappa}_0/\sigma_y$	1.15	1.13	1.06
σ_u/σ_y	1.81	1.61	1.22
$\zeta \cdot \varepsilon_y^2$	9.89×10^{-4}	1.52×10^{-3}	8.04×10^{-3}

3. FINITE ELEMENT FORMULATION

An elastoplastic analysis based on the finite element method[7], which takes into account the spread of plasticity through the cross-section and along the length of member, is employed in the analysis of steel compression members. In this approach, the member analyzed is divided into several elements along its length, and the cross-section is further subdivided into elemental areas, as shown in Fig. 2 for a hollow rectangular section. Each of the elemental areas is identified by, area dA_i, distance from the section centroid y_i, residual stress and strain, and stress-strain history. The incremental stress-strain relation for

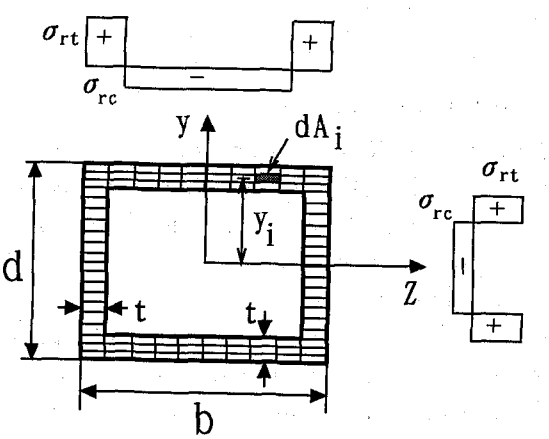

Fig. 2 Subdivision of section and residual stress distribution for a hollow rectangular section

each elemental area is described by the developed 2SM discussed in the previous section. In the following discussion the element formulation for beam-columns is briefly presented.

3.1 Beam-column element

The assumptions employed in the analysis are those of Bernoulli-Euler beam theory and the geometry within the element is interpolated from the nodal parameters using Hermitian cubic shape functions[7]. Local buckling is not considered in the analysis. The modified AULD of motion proposed by Jetteur *et al.*[14], is utilized in the element formulation. In this approach, beam elements are improved with the help of a Marguerre-type theory[19] which allows an introduction of initial deflections in the formulation and a reduction in the number of finite elements required to describe the nonlinear behaviour of the structure [14].

The stiffness equation and equivalent nodal force vector for the in-plane beam-column element in the local coordinate system was derived using the principle of virtual work. The stress resultants of axial force and bending moment are calculated simply by summing the contribution of each elemental area over the cross-section.

The Gauss-Lobatto numerical integration rule[20] is utilized in the present study to evaluate integrals in the stiffness equations. The number of sample points adopted is five. Once the stiffness matrix and nodal force vectors of each element are determined, they are transformed from the local to the global coordinate system using the usual transformation matrix. The full derivation of beam-column element is given in a work by Mamaghani et al.[1]

3.2 Solution scheme

The modified Newton-Raphson iteration technique coupled with the displacement control method is used in the analysis. The details of the solution procedure can be found in reference 21. The displacement convergence criteria is adopted in the analysis and the convergence tolerance is taken as 10^{-5}. It is assumed that the ratio of the Euclidean norm of the incremental nodal displacement vector in the current iteration to the maximum value of that in the previous iterations to be less than the convergence tolerance[21].

According to the algorithm discussed above, an elastoplastic beam-column finite element subroutine program was coded and implemented in the computer program FEAP[13] used in the analysis.

4. NUMERICAL RESULTS

The developed formulation was used to predict the experimentally determined hysteretic behaviour of several steel members, such as pin-ended columns and steel box columns of cantilever type subjected to cyclic loading. The results obtained are also compared with those from bilinear EPP, KH, and IH material models. The aim is to investigate the cyclic performance of the structural members and to compare the effect of each material model on the hysteretic behaviour.

Fig. 3 shows the uniaxial stress-strain relationship under monotonic loading for the two-surface model (2SM) and EPP, KH and IH material models. In the present study, based on the experimental results for SS400 steel[10], the kinematic and isotropic hardening rates are assumed as $E'_{st}/E = 1/84$, which is taken equal to the slope of the line joining the initial yield point to the loading point corresponding to 5% axial strain obtained by using the 2SM (see Fig. 3).

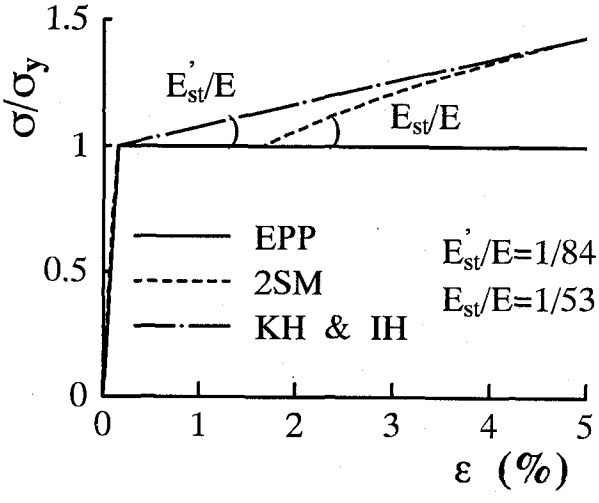

Fig. 3 Uniaxial stress-strain relationships for different material models under monotonic loading

4.1 Pin-ended columns

Pin-ended steel columns with solid rectangular section studied experimentally by Wakabayashi *et al.*[15] are analyzed by using the theory and numerical procedure described.

A typical example presented here is a column of length $L = 174\ mm$, width $b = 15.45\ mm$ and depth $d = 14.9\ mm$ subjected to cyclic axial load, as shown in Fig. 4. The slenderness ratio $\bar{\lambda}$ is 0.43, where $\bar{\lambda}$ is defined as[16)]

$$\bar{\lambda} = \frac{KL}{r}\frac{1}{\pi}\sqrt{\frac{\sigma_y}{E}} \tag{3}$$

in which L = length of the member; K = effective length factor; and r = radius of gyration for the cross section. The specimen is made of SS400 steel with the material properties of Young modulus $E = 207\ GPa$, yield stress $\sigma_y = 229\ MPa$ and yield plateau range $\varepsilon_{st}^{p} = 0.8\%$.

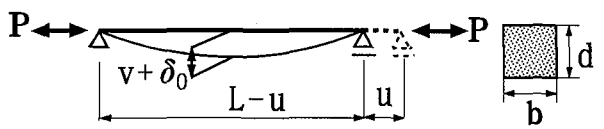

Fig. 4 Pin-ended column with a solid rectangular section ($\bar{\lambda} = 0.43$, $L = 174\ mm$, $b = 15.45\ mm$, $d = 14.90\ mm$)

An initial imperfection of $\delta(x) = \delta_0 sin(\pi x/L)$ is assumed in the analysis, where the initial deflection at midspan of the member δ_0, is taken as $0.001L$. In the analyses, ten elements are used to discretize the member along its length and the cross-section is subdivided into 14 layers. Compressive load is applied first and it is assumed to be positive.

Fig. 5 compares the normalized axial load P/P_y-axial displacement u/u_y and normalized axial load P/P_y-midspan deflection $(v+\delta_0)/d$ relationships while the normalized maximum compressive load P_{max}/P_y-number of cycles for the column is shown in Fig. 6. Here, P_y is the squash load; u_y is the yield displacement in tension for the column. Results obtained from experiment[15)] and analysis using the 2SM as well as the EPP, KH and IH material models.

With reference to Figs. 5 and 6, the following observation can be made. (1) The initial buckling load [see Figs. 5(a) and 6] is slightly higher in the experiment than that predicted by the analyses using different material models. This may be due to the experimental boundary conditions (unavoidable friction at the hinged supports) and the assumed initial imperfection in the analysis. (2) The significant features of the hysteretic loops

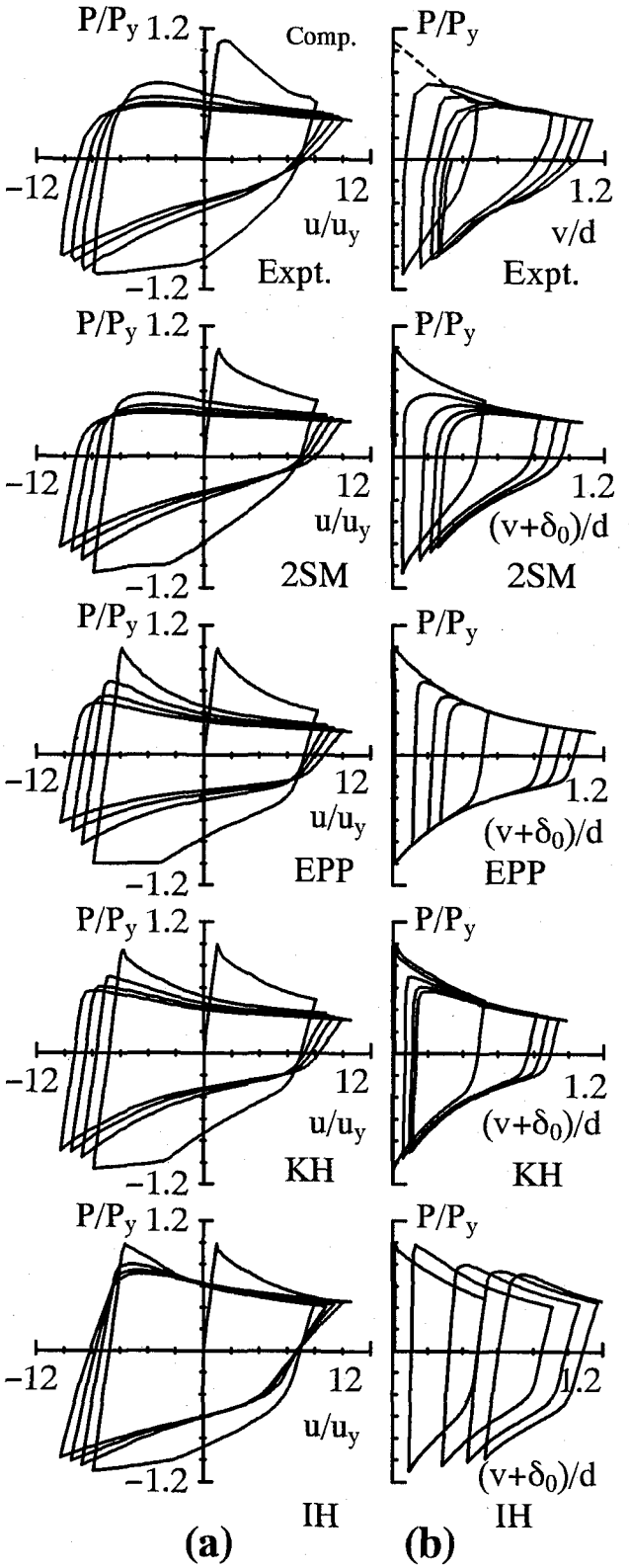

Fig. 5 Comparison between experimental and predicted hysteretic loops (Legend as in Fig. 4)

in Fig. 5(a) is that all of the models except the 2SM give the second and subsequent buckling load capacities higher than those of the experiment (see also Fig.6). The reasons are: (a) The

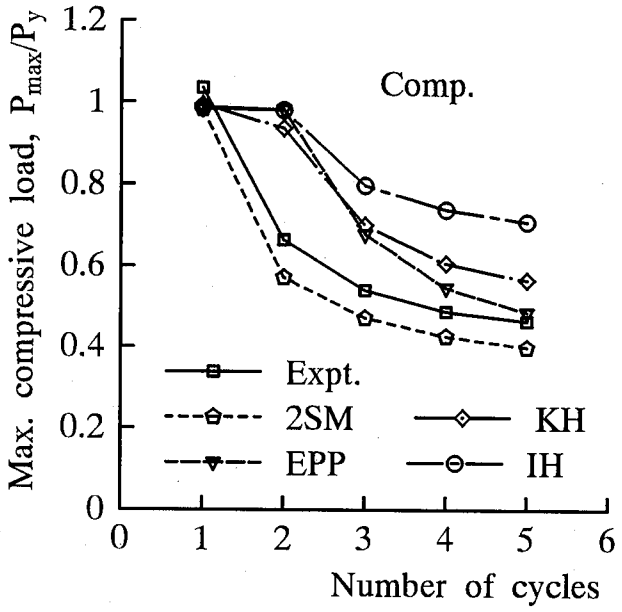

Fig. 6 Normalized maximum compressive load P_{max}/P_y-number of cycles for the pin-ended column with a solid rectangular section (Legend as in Fig. 4)

EPP and IH models do not consider the reduction of the elastic range due to plastic deformation (Bauschinger effect); and for the KH model the size of the elastic range is taken to be constant which does not represent the actual behaviour of structural steel[10]. In the case of the 2SM, Bauschinger effect is taken into account accurately through updating the size of yield surface as a function of EPS range[12] $\bar{\varepsilon}^p$, which has the effect of softening the hysteresis curve (reduction in stiffness), leading to a lower value of the buckling load capacity; (b) the 2SM correctly treats the yield plateau and cyclic strain hardening of the material. This leads to an accurate prediction of the axial load-midspan deflection [see Fig. 5(b)(2SM)] for the column, since the residual deflection of the column at the end of the previous tensioning has a large effect on the buckling load capacity and subsequent cyclic behaviour. As can be noticed from Fig. 5(b), the progress of buckling is different for each material model. In case of the IH model, in spite of large progress in buckling [see Fig. 5(b)], the buckling load does not decrease significantly due to the larger cyclic strain hardening. Similar results were obtained for the pin-ended columns with solid rectangular section of effective slenderness ratios $\bar{\lambda} = 0.85$ and 1.28 which are not presented in this paper.

Effect of residual stress and initial deflection: The effect of residual stress and initial deflection on the cyclic behaviour of steel members are examined using the developed formulation. As a typical example, the effect of longitudinal residual stresses produced due to welding, on the cyclic behaviour of a pin-ended column with a hollow rectangular section is shown in Fig. 7.

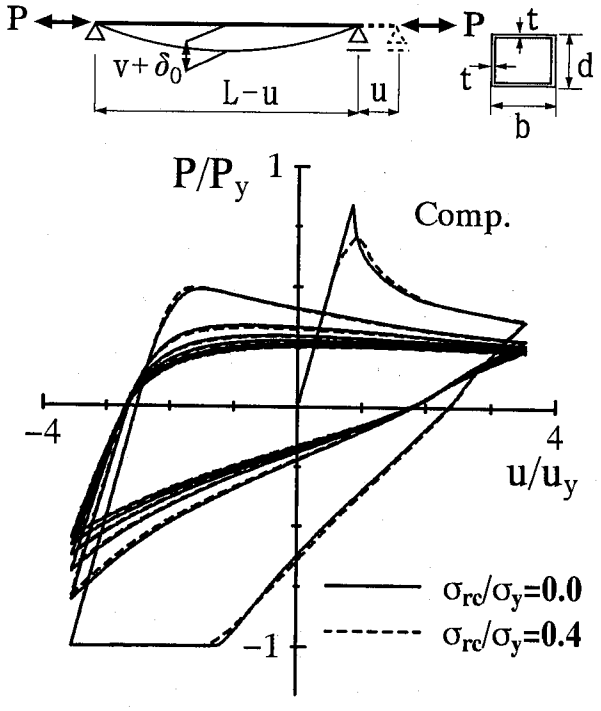

Fig. 7 Effect of residual stress ($\bar{\lambda} = 0.82$, $b = 150.0\ mm$, $d = 110.0\ mm$, $t = 4.5\ mm$, $\sigma_y = 266\ MPa$, $E = 197\ GPa$, $\varepsilon^p_{st} = 10\varepsilon_y$)

The member, of effective slenderness ratio $\bar{\lambda} = 0.82$, was subjected to cyclic axial loading. The material was assumed to be steel grade SS400. Ten elements were used to discretize the member along its length and the cross-section was subdivided into 30 (3×10) and 15 elemental areas in the flanges and webs, respectively (Fig. 2). The assumed residual stress distribution over the cross-section is also shown in Fig. 2 and is uniform along the entire length on the member. The tensile and compressive residual stresses are taken as $\sigma_{rt} = \sigma_y$ and $\sigma_{rc} = 0.4\sigma_y$, respectively.

The normalized axial load P/P_y-axial displacement u/u_y relationship, shown in Fig. 7, indicates that the initial buckling load capacity decreases by 15%, from $P/P_y = 0.84$ (corresponding $u/u_y = 0.85$) to $P/P_y = 0.71$ ($u/u_y = 0.91$), due to residual stresses. However, the residual stresses have almost no effect

on the subsequent cyclic behaviour of the column (Fig. 7).

From the mechanical point of view these observations can be explained as follows. Residual stresses cause the fibers with an initial compressive stress to yield before the applied load reaches the yield strength of the material. Then, yielding spreads progressively without significant strain hardening due to the existence of the yield plateau, as the load increases monotonically before unloading starts. Initially, this causes a reduction in compressive strength of the member, while later both of the response curves, with and without residual stress, almost coincide as can be seen in Fig. 7. At this stage, the residual stresses produced due to plastic deformation play a dominant role in the subsequent cyclic behaviour of the column as compared to the initial residual stresses.

Fig. 8 shows the effect of various initial deflections, namely, $\delta_0 = L/1000$ and $L/3000$, on the cyclic behaviour of the above described pin-ended column. The result in this figure shows that the increase in the initial deflection has only the effect of decreasing the initial buckling load capacity and does not affect subsequent cyclic behaviour.

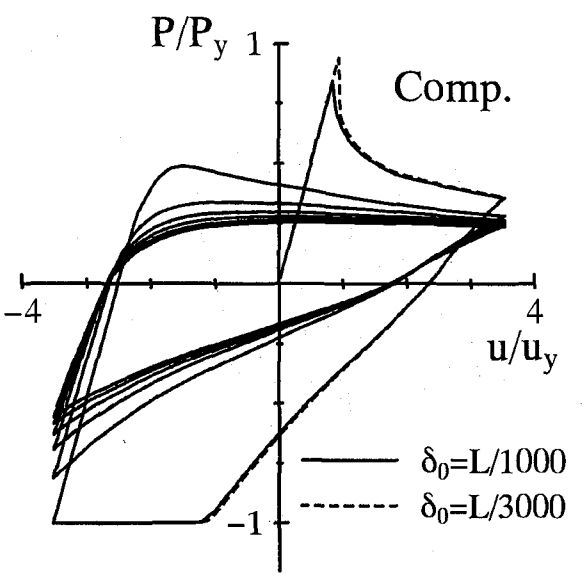

Fig. 8 Effect of initial deflection (Legend as in Fig. 7)

4.2 Steel box columns of cantilever type

With the rapid development of urban highway and bridge constructions, a large number of steel bridge piers of hollow box sections have been designed and constructed in Japan. They are normally designed as cantilever columns, see Fig. 9(a), or planar rigid frames. Since the performance of bridge piers under extreme loading conditions, such as severe earthquakes, is of great importance to prevent disruption of the urban transportation network, they must be designed to withstand such loading without collapse.

A great number of experimental investigations have been made on the inelastic cyclic behaviour of steel box columns modeling bridge piers in recent years[16),22)−24)]. However, accurate results can be obtained from analysis only by using a cyclic constitutive law representing the realistic behaviour of the material. In view of the above, a series of numerical studies on the cyclic behaviour of steel box columns are carried out using the developed formulation (2SM) and the results are compared with the test data[16)] as well as KH and IH material models. The results for a typical example (test UU11, Usami et al.[16)]) presented hereafter are intended to demonstrate the accuracy of the current implementation of the 2SM as well as the difference between use of the KH and IH material models.

The tested specimen has a slenderness ratio parameter of $\bar{\lambda} = 0.4$, width-thickness ratio parameter[16)] of $R_f = 0.3$, dimensions and boundary conditions as shown in Fig. 9(a). The parameter R_f inhibits local buckling of the flange and $\bar{\lambda}$ controls the global instability. It was subjected to a constant axial load of $P/P_y = 0.2$ and cyclic lateral displacement of increasing amplitude at the tip. The material used is steel SS400. Owing to the smaller value of R_f local buckling did not occur until loading point C in the last loop as shown in Fig. 9(b). Local buckling is not considered in the analysis and so the predicted results in Figs. 9(b) and 9(c) are valid up to the initiation of the local buckling at point C, see Fig. 9(b).

In the analysis, the specimen is divided into ten elements along its length and the cross section is subdivided into 8 and 17 layers parallel to the axis of bending for each flange and web, respectively. Initial geometrical imperfection and residual stress are not considered.

Hysteretic Behavior: The normalized lateral

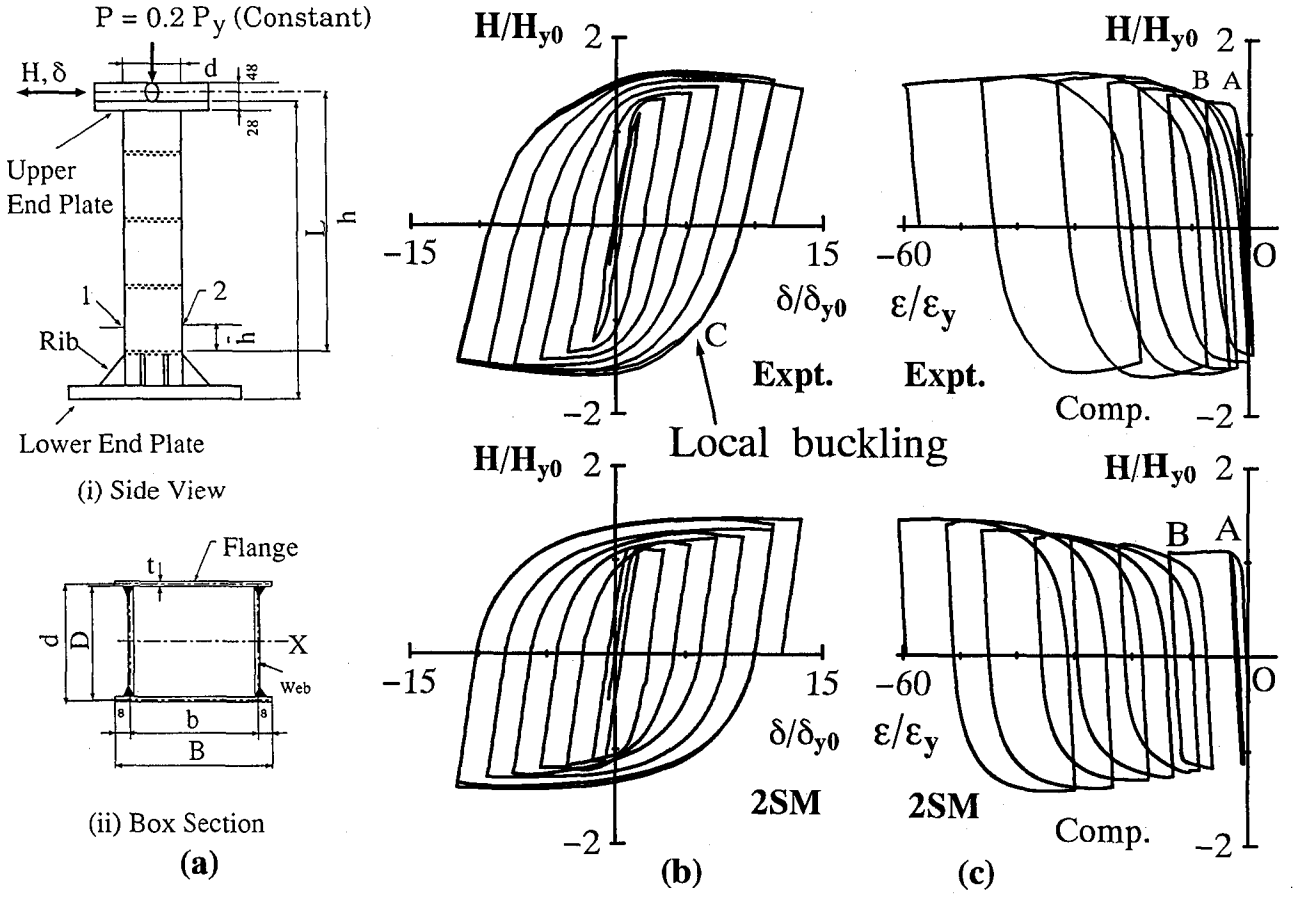

Fig. 9 Comparison between experimental (UU11[16]) and analytical (2SM) responses: a) specimen; b) normalized lateral load H/H_{y0}-lateral displacement δ/δ_{y0}; c) normalized lateral load H/H_{y0}-axial strain $\varepsilon/\varepsilon_y$ ($h = 853\ mm$, $B = 177\ mm$, $D = 127\ mm$, $t = 10.5\ mm$, $\bar{\lambda} = 0.4$, $R_f = 0.3$ and $\bar{h} = b/2$)

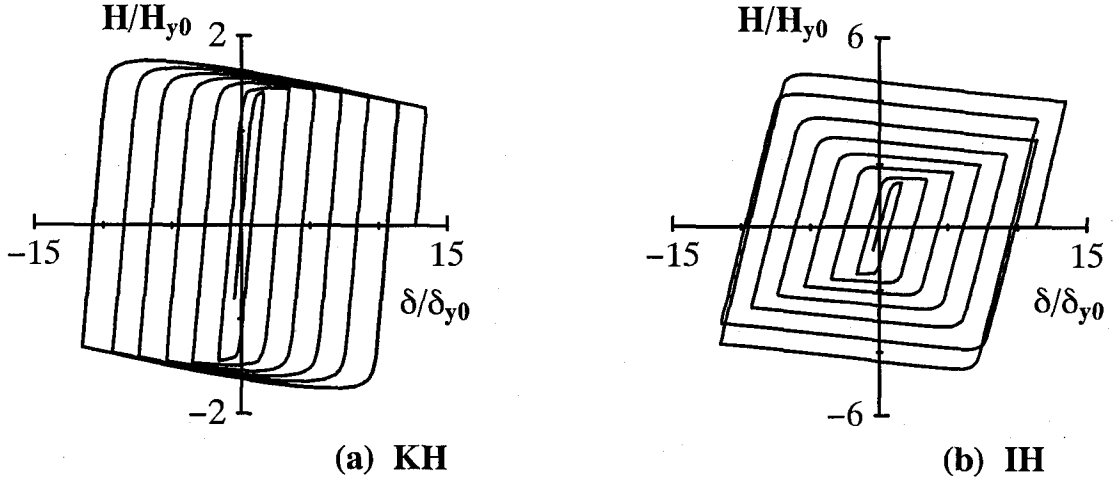

Fig. 10 Normalized lateral load H/H_{y0}-lateral displacement δ/δ_{y0} (Legend as in Fig. 9)

load H/H_{y0} versus lateral displacement δ/δ_{y0} and axial strain $\varepsilon/\varepsilon_y$ responses from the experiment and the 2SM are shown in Figs. 9(b) and 9(c). The axial strain is taken from the outer most fiber of the cross section at point 1 near the base of the column [see Fig. 9(a); $\bar{h} = b/2$]. The notations H_{y0} and δ_{y0} indicate, respectively, the yield load and yield displacement (neglecting shear deformation) corresponding to zero axial load[23].

From Figs. 9(b) and 9(c), it can be observed that the overall shape of the hysteresis loops from the developed formulation (2SM) are significantly closer to the experiments mainly owing to the accuracy of the 2SM. These results indicate that the developed formulation is accurate enough in both the material [see Fig. 9(c)] and structural [see Fig. 9(b)] levels. An observed small discrepancy between experimental and analytical (2SM) hysteresis loops is that the predicted cyclic load capacities [see Fig. 9(b)], in both directions of loading, are slightly lower than those of the experiment. The two possible reasons are: (1) The yield stress of welding material is much higher than that of steel SS400, which can lead the strength capacity to increase; (2) the length of yield plateau (ε^p_{st}) for the plate close to the weld may be reduced due to plastic deformation caused by welding, which in turns increases the strength capacity of the column. The second effect can be noticed by comparing the results in Fig. 9(c), in which the predicted axial strain along the envelope curve OAB is larger than that of the experiment.

One important point to notice is that, as shown in Fig. 9(c) for experiment, the axial strain increases in the direction of axial load (compression) due to lateral cycling of the specimen under constant axial load. This phenomena causes shortening of the plate components near the base of the column where the plastic deformation is large. Consequently, that may results a greater trend for local buckling to occur. Comparison between hysteresis loops in Fig. 9(c) shows that the developed formulation closely simulates the experimentally observed cumulative inelastic deformation or ratcheting during cyclic loading in the presence of constant axial load.

The corresponding normalized lateral load-displacement hysteresis loops obtained from the KH and IH material models are shown in Fig. 10. Comparison of the results in Figs. 9(b) and 10 shows that the lateral load carrying capacities, for each half-cycle, are over-estimated by both the KH model and, particularly, the IH model. Also these figures indicate that the overall shape of the hysteresis loops for the KH and IH grossly differ from those of the experiment and 2SM. Since as mentioned in the previous example, both the KH and IH models fail to represent accurately the real cyclic behaviour of steel SS400, such as the yield plateau, strong Bauschinger effect and cyclic strain hardening. It should be noted that the load axis in Fig. 10(b) is scaled up by three times compared to Figs. 10(a) and 9(b), to save the page space.

Energy absorption capacity: Energy absorption through hysteresis damping can reduce the amplitude of seismic response and, thereby, reduce the ductility demand on the structures. Therefore, it is one of the great interest in seismic design. In order to account for the displacement history to which the inelastic performance of a structure is highly sensitive, a normalized energy absorption , $\bar{E}$, defined as

$$\bar{E} = \frac{1}{E_y}\sum_{i=1}^{n} E_i \tag{4}$$

$$E_y = \frac{1}{2} H_{y0}\delta_{y0} \tag{5}$$

is considered to be a more objective measure of the cyclic inelastic performance of a member[23]. In which, E_i =energy absorption in the i-th half-cycle, n = number of half-cycles (here, one half-cycle is defined from any zero lateral load to the subsequent zero lateral load). Using the above definitions, Fig. 11 compares the normalized cumulative energy absorption capacity, $\bar{E}$ versus the number of half cycles n, obtained from experiment and analysis using the 2SM, KH and

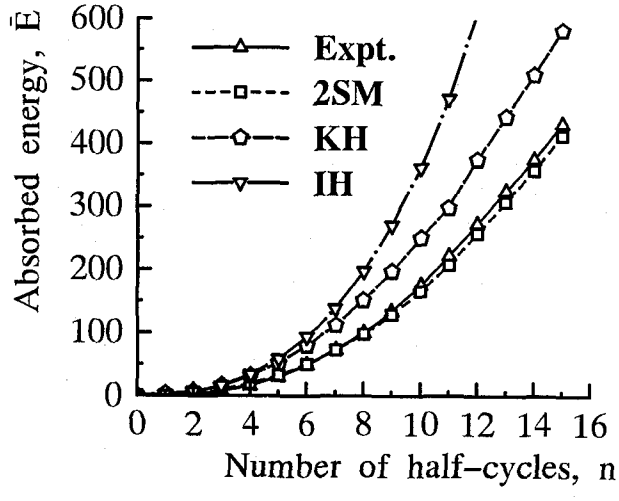

Fig. 11 Comparison between experimental (UU11[16]) and analytical responses; Normalized energy absorption capacity $\bar{E}$-number of half-cycles n

IH material models. From this comparison it is clear that the KH and IH material models grossly over-estimate the energy absorption capacity, especially as the number of cycles and displacement amplitude increase, in contrast to the good prediction of the 2SM.

In summary, the important conclusion is that the developed formulation (2SM) exhibits the capability of duplicating the experimental results more accurately, both quantitatively and qualitatively. Thus, it is recommended to use the developed formulation (2SM) where possible, since the EPP, KH and IH models may results in unrealistic estimates of the ductility and energy absorption capacity.

5. CONCLUSIONS

The present paper was concerned with the cyclic elastoplastic large displacement analysis of steel members, such as pin-ended columns and cantilever type of steel box columns modeling bracing members and bridge piers, respectively. An elastoplastic finite element formulation for beam-columns, accounting for both the material and geometrical nonlinearities, was developed and implemented in the computer program FEAP used in the analysis. The 2SM, recently developed by the authors, was employed for material nonlinearity.

The cyclic elastoplastic performance of the formulation was compared with the experimental results as well as with those obtained using the EPP, KH and IH material models. It was shown that:

- The formulation is applicable for any geometry of the cross-section and takes into account the spread of plasticity and history dependent parameters which are important for accuracy of analysis.
- The obtained results indicate that the reduction of the elastic range (Bauschinger effect) has a significant effect on the shape of the hysteresis loops and reduces the maximum compressive resistance under load reversals.
- The residual deflection (progress in buckling) of the pin-ended columns at the end of previous tensioning has a large effect on the reduction of the buckling load capacity and subsequent cyclic behaviour. This behaviour is accurately predicted by the developed formulation.
- The initial residual stress and an increase in the initial deflection significantly decrease the initial buckling load capacity and have almost no effect on the subsequent cyclic behaviour of the column.
- The proposed formulation accurately takes into account the important cyclic characteristics of axially loaded columns (bracing members), such as yielding in tension and buckling under compression, inelastic behaviour prior to buckling in compression , degradation of post buckling compressive resistance, deterioration of buckling load capacity in subsequent inelastic cycles, progressive degradation of tangent modulus during the cycles, and plastic elongation in the column length.
- The predicted hysteretic behaviour of structural steel members using the developed formulation (2SM) were in good agreement with the experimental results, both qualitatively and quantitatively, compared with the EPP, KH, and IH models.

Comparison between the experimental results and predictions indicates that these observations can be mainly attributed to the accuracy of the 2SM employed in the analyses. This leads to the conclusion that the 2SM is quite promising to account for the material nonlinearity of structural steels under cyclic loading. Therefore, it can be used in the nonlinear structural analysis; to generate parametric data; and to check the accuracy of more simplified models.

REFERENCES

1) Mamaghani, I. H. P., Usami, T. and Mizuno, E.: Inelastic large deflection analysis of structural steel members under cyclic loading, *Engng Struct.*, 1995, (accepted).
2) Soroushian, P. and Alawa, M. S.: Efficient formulation of physical theory brace models, *J. Struct. Engng, ASCE*, Vol. 114(11), pp. 2457-2473, 1988.
3) Maison, B. F. and Popov, E. P.: Cyclic response prediction for braced steel frames, *J. Struct. Engng, ASCE*, Vol. 106(7), pp. 1401-1416, 1980.
4) Boutros, M. K.: Nonlinear SDOF element for hysteretic analysis of pinned braces, *J. Engng Mech., ASCE*, Vol. 117(5), pp. 941-953, 1991.
5) Chen, W. F. and Han, D. J.: *Tubular members in offshore structures*, Pitman Publishing Inc, 1985.

6) Shibata, M. and Wakabayashi, M.: Mathematical expression of hysteretic behaviour of braces, (part 2, application to dynamic response analysis), *Transaction of the Architectural Institute of Japan*, No.320, pp. 29-35, 1982, (in Japanese).
7) Clarke, M. J.: Plastic-zone analysis of frames, *Advanced analysis of steel frames*, Edited by Chen, W. F. and Toma, S., CRC Press, Boca Raton, Fl, pp. 259-319, 1994.
8) Nakashima, M. and Wakabayashi, M.: Analysis and design of steel braces and braced frames in building structures, *Stability and ductility of steel structures under cyclic loading*, Edited by Fukumoto, Y. and Lee, G. C., CRC Press, Boca Raton, Fl, pp. 309-321, 1992.
9) Ishikawa, T., and Yoda, T.: Elasto-Plastic large displacement analysis of cyclically loaded axial members, *Proc. of 49th Annual Meeting, JSCE*, pp. 664-665, 1994.
10) Shen, C., Tanaka, Y., Mizuno, E. and Usami, T.: A two-surface model for steels with yield plateau, *J. Structural Engng/Earthquake Engng., JSCE*, Vol. 8(4), pp. 179-188, 1992.
11) Mamaghani, I. H. P., Shen, C., Mizuno, E. and Usami, T.: Cyclic behaviour of structural steels. I: Experiments, *J. Engng Mech., ASCE*, Vol. 121(11), pp. 1158-1164, 1995.
12) Shen, C., Mamaghani, I. H. P., Mizuno, E. and Usami, T.: Cyclic behaviour of structural steels. II: Theory, *J. Engng Mech., ASCE*, Vol. 121(11), pp. 1165-1172, 1995.
13) Zienkiewicz, O. C.: *The finite element method, 3rd Ed.*, McGraw-Hill, New York, 1977.
14) Jetteur, Ph., Cescotto, S., de Ville de Goyet, V. and Frey, F.: Improved nonlinear finite elements for oriented bodies using an extension of Marguerre's theory, *Computers and structures*, Vol. 17(1), pp. 129-137, 1983.
15) Wakabayashi, M., Nonaka, T., Koshiro, O. and Yamamoto, N.: An experiment on the behaviour of a steel bar under repeated axial loading, *Disaster preventation research institute annuals*, Kyoto University, Kyoto, Japan, No.14A, pp. 371-381, 1971, (in Japanese).
16) Usami, T., Itoh, Y., Mizutani, S., and Akoi, T.: Experimental study on the ductility of steel bridge piers under cyclic loading, *Research Report, Dept. of Civil Eng., Nagoya Univ.*, 1991.
17) Dafalias, Y. F. and Popov, E. P.: A model of nonlinear hardening materials for complex loading, *Acta. Mech.*, Vol. 21, pp. 173-192, 1975.
18) Chaboche, J. L., Dang-van, K. and Cordier, G.: Modelization of the strain memory effect on the cyclic hardening of 316 stainless steel." *Proc., 5th Int. Conf. on Struct. Mech. in Reactor Technol.*, Vol. L, Paper No. L11/3, Elsever, Amsterdam, The Netherlands, pp. 1-10, 1979.
19) Washizu, K.: *Variational methods in elasticity and plasticity', 3rd Ed.*, Pergamon Press, 1982.
20) Hughes, T. J. R.: *The finite element method,* Prentice-Hall Inc, New Jersey, 1987.
21) Mamaghani, I. H. P.: Cyclic elastoplastic behavior of steel structures: Theory and experiment, *A dissertation submitted to the Department of the Civil Engineering, Nagoya University, Nagoya, in partial fulfillment of the requirement of the degree of Doctor of Engineering*, March, 1996.
22) Ge, H. B. and Usami, T.: Development of earthquake-resistant ultimate strength design method for concrete-filled steel structures,*NUCE Research Report*, No. 9401, Nagoya Univ., Japan, 1994.
23) Usami, T., Mizutani, T. Aoki, Itoh, Y.: Steel and concrete-filled steel compression members under cyclic loading, *Stability and ductility of steel structures under cyclic loading*, Edited by Fukumoto, Y. and Lee, G. C., CRC Press, Boca Raton, Fl, pp. 123-138, 1992.
24) Watanabe, E., Emi, S., Isami, H. and Yamanochi, T.: An experimental study on strength of thin walled steel box beam-columns under repetitive bending, *Proc. of JSCE. Struct. Engng./Earthquake Engng., JSCE*, Vol. 5(1), pp. 43-57, 1988.

(Received September 18, 1995)